PHYSICAL REVIEW C VOLUME 21, NUMBER 4 APRIL 1980

0.8 GeV $p + {}^{208}$Pb elastic scattering and the quantity Δr_{np}

G. W. Hoffmann and L. Ray
University of Texas, Austin, Texas 78712
and Los Alamos Scientific Laboratory, Los Alamos, New Mexico 87545

M. Barlett and J. McGill
University of Texas, Austin, Texas 78712

G. S. Adams,* G. J. Igo, F. Irom, A. T. M. Wang, and C. A. Whitten, Jr.
University of California, Los Angeles, California 90024

R. L. Boudrie and J. F. Amann
Los Alamos Scientific Laboratory, Los Alamos, New Mexico 87545

C. Glashausser
Rutgers University, New Brunswick, New Jersey 08903

N. M. Hintz and G. S. Kyle†
University of Minnesota, Minneapolis, Minnesota 55455

G. S. Blanpied‡
New Mexico State University, Las Cruces, New Mexico 88003

(Received 5 November 1979)

Analyses of 0.8 and 1 GeV $p + {}^{208}$Pb elastic angular distribution data have obtained neutron-proton root-mean-square radius differences (Δr_{np}) which are not consistent. Therefore, the 0.8 GeV experiment was repeated using a high resolution spectrometer. The new higher precision data are consistent with the older data, apart from a 15% overall normalization difference. A second order Kerman-McManus-Thaler optical model analysis of the new data, using a model-independent neutron density, yields $\Delta r_{np} = 0.14 \pm 0.04$ fm, in good agreement with the most recent result obtained (0.16 ± 0.05 fm) from a similar analysis of the older 0.8 GeV data. In addition, the elastic angular distribution was extended to 42.5° center of mass in order to explore the momentum transfer region from 3.5 to 5.3 fm^{-1}. Although the familiar diffraction pattern persists to 42.5°, it was not possible within the framework of our application of the Kerman-McManus-Thaler optical model to fit the data even qualitatively at the larger momentum transfers.

NUCLEAR REACTIONS ^{208}Pb(p,p), $E = 0.8$ GeV, measured $\sigma(\theta)$; enriched target; resolution $\simeq 100$ keV, $\theta_{c.m.} = 2.5°$ to $42.5°$. Microscopic optical model analysis using KMT potential; deduced Δr_{np}; error analysis and comparison with other results.

I. INTRODUCTION

Results of the more recent analyses[1-4] of ~1 GeV proton-nucleus elastic scattering data obtained at Saclay,[5] Gatchina,[6] and the Los Alamos Clinton P. Anderson Meson Physics Facility (LAMPF)[7] suggest that for a given nucleus the value of Δr_{np}, the difference in root-mean-square (rms) radii of the neutron and proton matter density distributions, is reasonably well established, independent of the data analyzed or the details of the analyses. This favorable agreement between results obtained from 0.8 and 1 GeV analyses occurs in spite of the uncertain situation regarding the key nucleon-nucleon amplitudes which are used as input for the calculations.[3] It is also found[1-4] that the deduced Δr_{np} follow the trend of theoretical expectations, based, for instance on Hartree-Fock calculations.

However, a notable exception to this general agreement occurs for ^{208}Pb. All results[1,4,6] obtained from analyses of the 1 GeV Gatchina $p + {}^{208}$Pb data are consistent with $\Delta r_{np} = 0.0 \pm 0.07$ fm, while analyses of the 0.8 GeV LAMPF data suggest that $\Delta r_{np} > 0$; the most recent second order analysis[3] gives $\Delta r_{np} = 0.16 \pm 0.05$ fm. Theoretical predictions give $\Delta r_{np} > 0.11$ (see Table 21, Ref. 1); the Hartree-Fock results span the range 0.11–0.23 fm.

It is most likely, in light of the consistent results obtained from similar analyses of 0.8 and 1 GeV data for other nuclei, that the singular discrepancy in the deduced Δr_{np} for ^{208}Pb originates from the elastic data, since, as discussed below, uncertainties in the theoretical analyses cannot account for such a discrepancy.

At present the greatest source of uncertainty in 0.8 and 1 GeV proton-nucleus calculations are ambiguities in the nucleon-nucleon amplitudes. As explained in Ref. 3, the lack of both p-p and p-n triple scattering data at these energies permits, under certain assumptions, several discrete sets of spin-independent and spin-dependent nucleon-nucleon amplitudes which can lead to uncertainties in Δr_{np} for ^{208}Pb of about 0.15 fm. However, the 0.8 and 1 GeV analyses referred to above assume the same corresponding discrete p-p and p-n solutions. This is seen by comparing the parameters of the spin-independent amplitudes used in Refs. 1, 3, 4, and 6 with the discrete solutions given in Ref. 3 (Ref. 8) at 800 (1000) MeV. The good agreement between the results of most 0.8 and 1 GeV analyses implies that the dominant spin-independent nucleon-nucleon amplitudes assumed at these two energies are, if not accurate, at least consistent with each other. Assuming a particular discrete nucleon-nucleon solution, the uncertainty in Δr_{np} due to theoretical and amplitude uncertainties alone is ±0.05 fm (±0.03 fm) for first[2] (second[3]) order calculations. Thus, the large difference in Δr_{np} for ^{208}Pb between results of 0.8 and 1 GeV analyses (~0.15 fm) cannot be accounted for by theoretical or nucleon-nucleon amplitude uncertainties, and one expects that either the 0.8 or the 1 GeV data are wrong.

Relatively small systematic errors in the determined laboratory scattering angle and relative normalization of the angular distribution data could account for the discrepancy seen between the results of analyses of the 1 and the 0.8 GeV $p+^{208}$Pb data, since accurate determination of these quantities is crucial to a reliable determination of Δr_{np}. Optical model calculations, using a first order microscopic potential, generated as prescribed by Kerman-McManus-Thaler (KMT)[9] from nucleon-nucleon scattering amplitudes and neutron and proton densities characterized by Fermi distributions, can estimate the sensitivity of Δr_{np} to such errors. For $p+^{208}$Pb at ~1 GeV, it is found that changing the neutron radius parameter by an amount which changes $\langle r_n^2\rangle^{1/2}$ (the neutron rms radius) by ±0.1 fm shifts the positions of the second, third, and fourth minima in the angular distribution by ±0.05, ±0.07, and ±0.13 degrees, respectively; this is expected from diffraction model arguments. Changing the diffuseness by an amount sufficient to change $\langle r_n^2\rangle^{1/2}$ by ±0.1 fm does not change the positions of the maxima or minima, but rather changes the overall slope of the angular distribution by ~±0.8%/degree. First and second order analyses[2,3] of the LAMPF data incorporated these absolute angle and normalization uncertainties into the quoted errors for Δr_{np}. It is not clear whether this was done for any of the published analyses[1,4,6] of the Gatchina data.

Because of the extreme interest in Δr_{np} for ^{208}Pb, and because ^{208}Pb is the only case with conflicting results for Δr_{np} arising from independent analyses of medium energy proton elastic scattering data obtained at different laboratories, the 0.8 GeV LAMPF experiment was repeated. In addition to retaking the data from 2.5°–31.0°, the elastic angular distribution was extended to 42.5° (center of mass) in order to explore the momentum transfer region from 3.5 to 5.3 fm^{-1}.

As discussed in Secs. II and III, all errors associated with the new data are about half as large as those of the previous LAMPF data, and the two data sets are consistent to within the quoted uncertainties. The results of a second order KMT analysis of the new data are discussed in Sec. IV, where a value of $\Delta r_{np}=0.14\pm0.04$ fm is obtained; the error represents the contributions of all known uncertainties (assuming a particular discrete set of nucleon-nucleon amplitudes; see Ref. 3).

II. EXPERIMENTAL

The data were obtained, as before,[7] using the high resolution spectrometer (HRS) at LAMPF. A 19.7 mg/cm² (±1%) foil was used for angles less than 31°, while a 150 mg/cm² (±1%) foil was used for the larger angles. The energy resolution was typically 100 keV (150 keV) for the thin (thick) target. The beam energy was determined to be 800 ± 0.5 MeV by utilizing the known line integrals of the magnetic fields of the HRS dipoles and by simultaneous measurements on the EPB Channel using the technique of laser dissociation of H^- ions.[10]

The overall experimental angular resolution ($\Delta\theta$) was determined to be $\simeq$2 mr full width at half maximum (FWHM) from the observed energy resolution for $p+p$ elastic scattering, since for this case the resolution is dominated by the kinematic term $(dE/d\theta)\Delta\theta$. Two quantities contribute in quadrature to $\Delta\theta$: the divergence of the beam on target and the angular resolution of the HRS itself. The angular resolution of the HRS was determined to be $\leq$1.5 mr through an angle calibration procedure which used five tantalum slits (width of opening 0.7 mr and separation 6.7 mr) placed in front of the HRS about 1 m from the target. Thus the angular divergence of the beam was also about 1.5 mr (FWHM).

The absolute scattering angle was determined to ±0.02° through extensive measurements on both sides of the beam line over the angular interval 8°–12° and also by direct observation of the beam on the focal plane with the HRS set at 0°. For the left-right 8°–12° measurements, the data were sorted into ≃0.1° angle bins and for each bin the ratio of counts in the 0^+ elastic peak to those in the 2.7 MeV 3^- inelastic peak was computed. Since the $0^+/3^-$ ratios are independent of normalization and show considerable structure over the angular region considered, a comparison of the results obtained from both sides of the beam line made it possible to determine absolute scattering angle to 0.02°. After the absolute angle was calibrated in this way, the HRS was set at 0°, and a low-intensity, pencil beam was run through the spectrometer and observed on the focal plane with the usual focal plane detection system. The calculated "scattering angle" at the target for these "unscattered" beam particles was consistent with 0, and thus provided an independent check of the absolute angle calibration. A beam profile monitor (resolution ±0.25 mm) located in the 2 m diameter scattering chamber was used to check the horizontal beam position on target before and after each run. The horizontal beam position on target was maintained to ±0.5 mm during the experiment. The optics of the beam line are such that this uncertainty translates to less than 0.01° uncertainty in beam angle on target.

Absolute focal plane proton-event trigger efficiency for the region of the elastic events was determined to be 0.95 ± 0.01 by running an 800 MeV (2000 protons/sec) pencil beam through the HRS at 0° and evaluating the quantity (BEAM and INTERRUPT)/BEAM. A BEAM event was defined as a fourfold coincidence among three drift chambers and a thin (0.25 mm) scintillator located on the beam optic axis at the center of the HRS scattering chamber, while INTERRUPT (the actual event trigger for the PDP 11/45 data acquisition computer) represented a fourfold coincidence among the four large focal plane scintillators. Efficiency defined in this way, besides including actual scintillator efficiencies, also takes into account attenuation in the focal plane scintillators (as well as attenuation due to the thin mylar window at the exit of the HRS and the air and drift/delay-line chambers located before the last INTERRUPT defining scintillator). Beam attenuation in the BEAM defining detectors was calculated to be less than 0.1%.

Three small test scintillators located before, between, and after the interrupt defining scintillators (on optic axis of HRS) were then used during the course of the experiment to monitor on-line the trigger efficiency. The ratio (INTERRUPT and TEST)/TEST, where TEST signified a threefold coincidence among the test counters was always >0.998. Since, by definition, a test coincidence meant that the trajectory passed through all four interrupt scintillators, this result implied that the apparent 5% event trigger inefficiency was due entirely to attenuation. Also, since the test counters were about ten times smaller than the interrupt counters, it was evident from the test results that there were no rate dependent effects, even for the larger angles where beam currents of ~50 nA were used and the instantaneous singles rates in some of the interrupt counters were as large as 0.5×10^6/sec (due mainly to room background). In addition, many studies of the trigger efficiency versus singles rates in the scintillators have been made over the past several years, and the conclusion based on these studies is that there are no rate effects as long as instantaneous singles rates are $\lesssim 0.5 \times 10^6$/sec. Other correction factors are discussed in the next two paragraphs.

The overall efficiency of the delay-line and drift chambers used to record, for each event, trajectory position and angle information at the focal plane was determined for each run by evaluating the quantity: [good proton particle identification (as determined from pulse height and time-of-flight information from the large focal plane scintillators[11]) *and* good chamber time-sum-checks[12]]/(good proton particle identification). The chambers occupied a region in space which was larger than the region occupied by the scintillators. The overall chamber efficiency was typically 80–90% (±2%).

The correction for real events missed due to computer dead time was determined for each run by evaluating the quantity INTERRUPT (computer not busy)/INTERRUPT (computer busy *or* not busy). Depending upon the interrupt rate this quantity typically varied from ~0.4 to ~1. Experience with the HRS over the past several years has indicated that this correction factor is reliably determined to better than 1%.

For each run at angles greater than 12° the relative integrated beam current was determined with an ion chamber (IC) and a secondary emission monitor (SEM) located 1 m and 3 m, respectively, downstream from the target. Only the IC was used at smaller angles. The IC/SEM ratios were constant to ±1.5% during the course of the experiment. After spanning 2.5°–30° in 1.5° steps, as an additional check on the relative normalization, three angles (5.5°, 12.5°, and 19.5°) were repeated in quick succession, and the data were reproduced to within statistics.

The absolute gain of the ion chamber was determined by placing it in front of the EPB Faraday cup,[13] whose calibration is reported accurate to ~1%, and comparing the integrated charge recorded by both devices. The ion chamber gain determined in this way agreed (to within 2%) with the calculated value.

An absolute normalization of the data was obtained at 12° using a 3 mm thick (~5 MeV energy loss) rectangular tantalum aperture of solid angle 0.73 msr (±1%) located about 1 m from the target in front of the HRS. The HRS angular acceptance is uniform over 2.5 msr. The average cross section for elastically scattered protons passing through the aperture was determined from the known solid angle, beam current, target thickness and appropriate correction factors discussed above. By integrating the relative differential cross section (obtained without the aperture) over the region defined by the aperture, the absolute normalization was obtained. Because the aperture defined the center portion of the maximum in the angular distribution at ~12%, little error (~1%) was introduced into the normalization due to uncertainty in the actual space scattering angle defined by the aperture. Taking all uncertainties into account, absolute normalization error is believed to be ~±5%.

III. RESULTS

The new data obtained in this experiment, along with a theoretical curve to be discussed, are shown in Fig. 1. As seen in the figure, the familiar diffraction pattern persists over 10 decades and contains 10 oscillations. Statistical errors in the data are typically less than 1% for angles less than 22°, 2% from 22°–30° and increase to ~35% for the largest angles (large angle errors also include background subtraction). The statistics, absolute/relative normalization and absolute scattering angle determination associated with the new data are each about a factor of 2 better than obtained for the earlier 0.8 GeV data reported in Ref. 7.

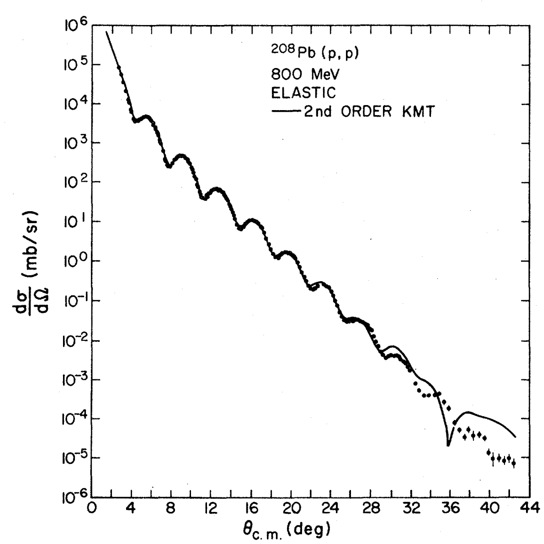

FIG. 1. The new 0.8 GeV $p+^{208}$Pb elastic angular distribution data are compared (solid curve) with the result of the second order KMT analysis discussed in text.

The absolute normalization (±5%) of the new data presented here is 15% larger than that of Ref. 7 (quoted to ±15%). The earlier data[7] were normalized relative to H(p,p) elastic data obtained with a CH target and then normalized relative to the H(p,p) data of Willard, et al.[14] Experience with the HRS has shown that particular care must be exercised with the H(p,p) cross normalization procedure because the large $dE/d\theta$ associated with p-p scattering causes the elastic events to occupy an extended region in the dispersion direction of the focal plane, which is not the case for any target heavier than carbon. It is known that the HRS relative solid angle varies by as much as 10% depending upon focal plane position.

Apart from the 15% normalization difference, the old and new 0.8 GeV $p+^{208}$Pb elastic angular distributions are consistent over the region of overlap. In particular, the positions of the minima and maxima, as well as the relative slopes, agree to within the stated uncertainties.

IV. THEORETICAL

Only a brief description of the method of analysis will be given, since the technique and approach used here are identical to those described in detail elsewhere.[2,3]

The analysis begins by generating the spin-dependent microscopic optical potential of KMT[9] from proton-nucleon scattering amplitudes and the one-body point-proton and -neutron densities describing the target nucleus. The major second order terms in the proton-nucleus optical potential which arise from target nucleon correlations are included as perturbations to the first order potential.[3] The two-nucleon parameters used, as well as the point-proton density for ^{208}Pb, are the same as those given in Ref. 3. As discussed there, the proton density is obtained from the empirical charge density by taking into account corrections which arise from the electric and magnetic form factors of both protons and neutrons [see Eq. (13) of Ref. 3].

For the initial model-dependent analysis, the three parameter Gaussian (3pG) form

$$\rho_n(r)=\rho_0(1+w_n r^2/R_n{}^2)/\{1+\exp[(r^2-R_n{}^2)/z_n{}^2]\} \tag{1}$$

was assumed for the neutron distribution. The resulting microscopic optical potential thus had three adjustable parameters (w_n, R_n, and z_n) which were searched to optimize the fit to the cross section data, over the angular range 2°–25°, through solution of the Schrödinger equation with relativistic kinematics.[15] The fit to the data is shown as the solid curve in Fig. 1. The fit is excellent out to about 30°, quantitatively reproducing the features of the data which are important for determining the neutron density distribution: the positions of the maxima and minima and the overall relative slope of the angular distribution. Beyond 30° the theory abruptly fails to resemble the data even qualitatively. This failure, which is not a consequence of omitting the larger angle data in the fitting procedure, is commented upon in Sec. V, and does not affect the conclusions regarding the deduced neutron density distribution but rather provides incentive for further theoretical work. The elastic analyzing power data[16] were also adequately reproduced as given in Refs. 2 and 3.

Table I gives the best fit parameters of the 3pG model density, as well as the deduced neutron and the known proton rms radii. The quantity Δr_{np}, the neutron-proton rms radius difference, is seen to be 0.14 fm, which is to be compared to $\Delta r_{np}=0.16$ fm obtained from a similar analysis[3] of the earlier 0.8 GeV data.[7]

However, as discussed in Refs. 2 and 3, application of the above procedure for determining $\langle r_n^2\rangle^{1/2}$ and Δr_{np} introduces errors into the derived results which necessarily (1) reflect the uncertainties associated with the nucleon-nucleon amplitudes, (2) are model dependent, and (3) depend upon systematic errors in the data. Each of the above must be considered before making quantitative statements about the accuracy of the derived results. Such considerations lead to the second stage of the analysis in which these errors are explicitly calculated or estimated.

The error introduced into $\langle r_n^2\rangle^{1/2}$ due to uncertainties in the nucleon-nucleon scattering amplitudes at 800 MeV is discussed in detail in Ref. 3 where it is shown that an error of ±0.03 fm is expected, assuming a particular discrete nucleon-nucleon solution. The error in the deduced neutron rms radius due to experimental error in beam energy determination and the absolute normalization and scattering angle of the data was determined by altering the data within the limits of uncertainty and recovering the original fit by variation of the neutron density. In the order mentioned above, the contributions are ±0.006 fm, ±0.009 fm, and ±0.018 fm.

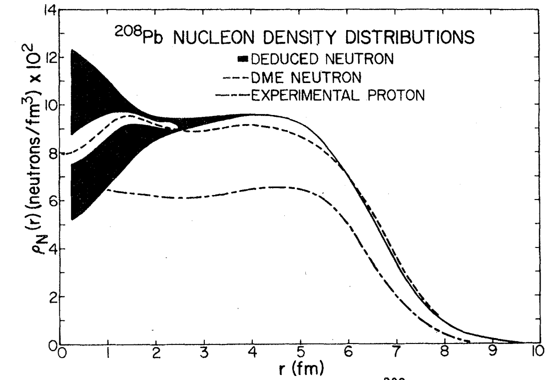

FIG. 2. Point-nucleon densities for ^{208}Pb. The shaded band represents the error envelope obtained from the model-independent analysis discussed in text. Shown also are the DME point-neutron density (dashed curve) and the point-proton density (dash-dot curve) inferred from electron scattering results.

The error due to model dependence and the statistical error in the angular distribution data was estimated by generating an error envelope using approximately model-independent neutron densities as described in Refs. 2 and 3. The resulting error envelope is shown in Fig. 2, where it is compared with a typical Hartree-Fock prediction[17] for the ^{208}Pb neutron density. Also shown in Fig. 2 is the point-proton density as determined from the results of electron scattering experiments. From these calculations it was determined that the model dependence and statistical errors contribute ±0.008 fm to the uncertainty in $\langle r_n^2\rangle^{1/2}$. The mean, $\bar{\rho}_N(r)$, and standard deviation $\Delta\rho_{N,st}(r)$, of

TABLE I. Results of analysis of new 0.8 GeV $p+{}^{208}$Pb elastic angular distribution data. The first three entries give numerical values of the parameters of Eq. (1) of the text. The root-mean-square (rms) radii for the point-nucleon density distributions are $\langle r_n^2\rangle^{1/2}$ and $\langle r_p^2\rangle^{1/2}$, and $\Delta r_{np}=\langle r_n^2\rangle^{1/2}-\langle r_p^2\rangle^{1/2}$. The quantity $\langle r^2\rangle_{\rm CH}{}^{1/2}$ is the rms radius of the charge form factor taken from electron scattering. See text for discussion of error on Δr_{np}. Listed under Δr_{np} theory are Hartree-Fock results. DME is the density-matrix-expansion approach described in Ref. 17.

	This analysis							Δr_{np} theory	
w_n	R_n (fm)	z_n (fm)	$\langle r_n^2\rangle^{1/2}$ (fm)	$\langle r_p^2\rangle^{1/2}$ (fm)	$\langle r^2\rangle_{\rm CH}{}^{1/2}$ (fm)	Δr_{np} (fm)	DME [a] (fm)	Other HF [b] (fm)
0.440	6.21	3.04	5.593	5.453	5.503	0.14 ± 0.04	0.20	0.11 – 0.23

[a] Reference 16.
[b] Reference 1.

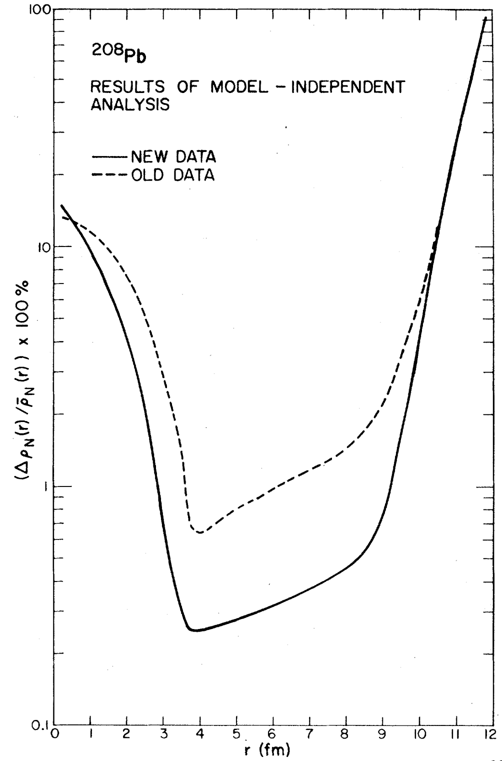

FIG. 3. The solid curve is the uncertainty in the ^{208}Pb neutron density as a function of radial position as determined from the model-independent analysis of the new 0.8 GeV $p+{}^{208}$Pb elastic angular distribution data. The dashed curve is the same uncertainty as obtained from an identical analysis of the earlier 0.8 GeV data.

the random densities which define the error envelope were also determined. Shown in Fig. 3, as the solid curve, is $\Delta\rho_{N,st}(r)/\bar{\rho}_N(r)\times 100\%$. Figure 3 clearly suggests that the entire surface region is accurately probed through the model-independent analysis.

It is interesting to compare the present error envelope with one generated from the earlier data, shown in Fig. 3 as the dashed curve. The factor of 3 improvement in results is directly related to the smaller statistical errors associated with the new data.

Considering all errors discussed as independent leads to a total uncertainty in $\langle r_n^2\rangle^{1/2}$ (and also Δr_{np}) of ± 0.04 fm. Uncertainties in the nucleon-nucleon amplitudes account for most of this error.

V. SUMMARY AND CONCLUSIONS

The 0.8 GeV $p+{}^{208}$Pb elastic angular distribution was remeasured using the HRS at LAMPF because of the discrepancy in results for Δr_{np}, the neutron-proton rms radius difference, deduced[1-4] from the Gatchina 1 GeV data[6] and the earlier 0.8 GeV LAMPF data.[7] In all respects the new LAMPF data are substantially better than the data reported earlier. Particular care was exercised in determining the absolute angle, relative slope, and absolute normalization of the angular distribution.

The new data (consistent with the earlier data to within the quoted uncertainties) were analyzed using the spin-dependent microscopic optical potential of KMT[9] and a model-independent approach.[2,3] Second order terms in the proton-nucleus optical potential were included, and all known contributions to errors in the deduced Δr_{np} were considered. A final value of $\Delta r_{np}=0.14\pm 0.04$ fm was obtained, in good agreement with $\Delta r_{np}=0.16\pm 0.05$ fm obtained through a similar analysis[3] of the earlier data, but in disagreement with the results (0.0 ± 0.07 fm) obtained[1,4,6] through analysis of the Gatchina data. The error of ± 0.04 fm is dominated by uncertainties in the nucleon-nucleon scattering amplitudes at 0.8 GeV. Future experiments are planned at LAMPF which will help determine these parameters better.

The 1 GeV analyses[1,4,6] apparently do not consider the contribution of experimental uncertainties to the errors assigned to Δr_{np}. For example, as discussed in Sec. I, a 0.05° error in determining the absolute scattering angle will change the deduced Δr_{np} by almost 0.1 fm. It is therefore crucial to assign realistic errors to the results of the 1 GeV analyses in order to resolve the discrepancy for Δr_{np} of ^{208}Pb.

In addition to retaking the data between 2° and 30°, the elastic angular distribution was extended to 42.5° in order to explore the momentum transfer region, 3.5–5.3 fm^{-1}. It was observed that the familiar diffraction pattern persisted to 5.3 fm^{-1}, but that the theory did poorly at the large momentum transfers. It was not possible to fit the larger angle data through adjustment of any of the input parameters. The apparent breakdown in theory between 30° and 42° can be traced to the accidental cancellation between the Coulomb and nuclear amplitudes at about 35° and is presently under investigation.[18]

This research was supported in part by the U.S. Department of Energy, The Robert A. Welch Foundation, and the National Science Foundation.

*Present address: Bates Laboratory, Massachusetts Institute of Technology, Cambridge, Massachusetts 02139.

†Present address: SIN, 5234 Villigen, Switzerland.

‡Present address: University of South Carolina, Columbia, South Carolina 29208.

[1]A. Chaumeaux, V. Layly, and R. Schaeffer, Ann. Phys. (N.Y.) 116, 247 (1978).
[2]L. Ray, W. R. Coker, and G. W. Hoffmann, Phys. Rev. C 18, 2641 (1978).
[3]L. Ray, Phys. Rev. C 19, 1855 (1979).
[4]G. K. Varma and L. Zamick, Phys. Rev. C 16, 308 (1977).
[5]R. Bertini *et al.*, Phys. Lett. 45B, 119 (1973).
[6]G. D. Alkhazov *et al.*, Leningrad Report No. LINP-244, 1976 (unpublished).
[7]G. S. Blanpied *et al.*, Phys. Rev. Lett. 39, 1447 (1977).
[8]L. Ray, Phys. Rev. C 20, 1857 (1979).
[9]A. K. Kerman, H. McManus, and R. M. Thaler, Ann. Phys. (N.Y.) 8, 551 (1959).
[10]D. A. Clark *et al.*, Particle Acceleration Conference, 1979, San Francisco, California (unpublished).
[11]G. S. Blanpied, Ph.D. thesis, University of Texas at Austin; Los Alamos Sci. Laboratory Report No. LA-7262-T, 1978 (unpublished).
[12]C. L. Morris and G. W. Hoffmann, Nucl. Instrum. Methods 153, 599 (1978); C. L. Morris, G. W. Hoffmann, and H. A. Thiessen, IEEE Trans. Nucl. Sci. NS-25, No. 1, 1978.
[13]R. J. Barrett *et al.*, Nucl. Instrum. Methods 129, 441 (1975).
[14]H. B. Willard *et al.*, Phys. Rev. C 14, 1545 (1976).
[15]W. R. Coker, L. Ray, and G. W. Hoffmann, Phys. Lett. 64B, 403 (1976).
[16]G. W. Hoffmann *et al.*, Phys. Rev. Lett. 40, 1256 (1978).
[17]J. W. Negele and D. Vautherin, Phys. Rev. C 5, 1472 (1972); the DME code of Negele provided the numerical results given here.
[18]L. Ray, G. W. Hoffmann, and R. M. Thaler (unpublished).